A CHALLENGING TEST CASE FOR LARGE EDDY SIMULATION: HIGH REYNOLDS NUMBER CIRCULAR CYLINDER FLOW

Michael Breuer
Institute of Fluid Mechanics, University of Erlangen–Nürnberg
D–91058 Erlangen, Germany

ABSTRACT

A thorough numerical investigation of high Reynolds number ($Re = 140,000$) circular cylinder flow was performed based on large eddy simulation (LES). The objective was to evaluate the applicability of LES for practically relevant high–Re flows and to investigate the influence of subgrid scale modeling and grid resolution on the quality of the predicted results. Because the turbulent von Kármán vortex street past circular cylinders involves most of the characteristic features of technical applications, it is an ideal test case for this purpose. Based on a parallelized finite volume Navier–Stokes solver, computations were carried out on a series of grids applying both the Smagorinsky and the dynamic subgrid scale model. The simulations yielded information on the time–averaged flow field, the resolved Reynolds stresses and integral parameters such as drag coefficient, recirculation length and Strouhal number. The results were analyzed in detail and compared with experimental data.

INTRODUCTION

The long–term objective of the present work is to develop a large eddy simulation (LES) technique which is able to simulate high Reynolds number flows of practical relevance, especially bluff body flows. In order to reach this goal, it is necessary to validate the physical model and the numerical method applied for LES by detailed investigations based on well–documented test cases. The necessity to place such test cases at the disposal of the LES community was recognized some years ago, e.g. by Rodi et al. (1997) and Voke (1997). The most recent initiative in this direction was originated by the Advisory Group for Aerospace Research and Development (AGARD), which published a selection of test cases especially for the validation of LES codes (AGARD–AR–345, 1998). Flows of different types and complexities are provided starting with homogeneous isotropic turbulence and ending with four complex flow problems. One of these more challenging test cases is the flow past a circular cylinder. Especially at high Reynolds numbers such as that in the present investigation ($Re = 140,000$), the cylinder flow can be considered as the paradigm of complex flows, because it involves remarkably complex flow features such as thin separating shear layers, transition and large–scale vortex motion in the wake. Therefore, successful applications for this test case can be considered as the *ticket to real world applications* of LES. Another advantage of using this flow as a test case is given by the detailed and well–documented experiment performed by Cantwell and Coles (1983), who recorded time–resolved and time–averaged data for the Reynolds number computed. In a previous study by the author (Breuer, 1998b), LES results based on the Smagorinsky model only were evaluated for cylinder flow. The present paper is an extension to dynamic subgrid scale modeling in order to gain experience with high–Re complex flows for this model and to compare the performance of both models for different grid resolutions.

COMPUTATIONAL METHOD AND MODELS

A 3–D finite–volume incompressible Navier–Stokes solver for arbitrary non–orthogonal and non–staggered grids ($\mathcal{LESOCC}$ = $\mathcal{L}$arge $\mathcal{E}$ddy $\mathcal{S}$imulation $\mathcal{O}$n $\mathcal{C}$urvilinear $\mathcal{C}$oordinates) was applied. Recently, the code was extended by a multi–block structure strongly improving the possibility of resolving complex geometries. Furthermore, the multi–block implementation was also the basis for parallelization by domain decomposition and message passing (MPI). $\mathcal{LESOCC}$ is highly vectorized, allowing efficient computations especially on vector–parallel machines such as the NEC SX–4 or Fujitsu VPP 700. Details about all features of $\mathcal{LESOCC}$ were given by Breuer and Rodi (1994, 1996), and Breuer (1998a). In the present study spatial discretization is based on central differences of 2nd order accuracy (CDS). A low–storage Runge–Kutta method

(2nd order accurate) is applied for time marching. For all computations shown in this paper, a dimensionless time step $\Delta t = 2\times10^{-4}$ is chosen. Two different subgrid scale (SGS) models are used, namely the Smagorinsky model with Van Driest damping and a dynamic SGS model based on the ideas of Germano et al. (1991) and Lilly (1992).

DESCRIPTION OF THE TEST CASE

The investigation of LES for flows past circular cylinders was started with a low (sub–critical) Reynolds number $Re = 3900$. In the course of this validation process detailed investigations on different numerical and modeling aspects influencing the quality of LES solutions have been performed (Breuer, 1998a). The present paper concentrates on the high Reynolds number case of $Re = 140,000$. At this Reynolds number the flow is still sub–critical, i.e. the boundary layers at the cylinder separate laminarly and transition takes place in the free shear layers. In the wake strong vortex shedding is observed. Compared with the low–Re case the boundary layer is about six times thinner ($\delta \sim 1/\sqrt{Re}$). Nevertheless, to avoid any kind of wall functions, the boundary layer is resolved by extremely fine grids in the near–wall region and no–slip boundary conditions are applied (see Fig. 1 (c)). In the spanwise direction of the cylinder periodicity of the flow is assumed and a constant velocity profile (zero turbulence level) is imposed at the inflow plane. At the outflow a convective boundary condition is applied (Breuer, 1998a).

Primarily, two different curvilinear O–type grids have been used (see Table 1). The first is a '*coarse*' grid (named **A**) with 165×165 control volumes (CV) in the cross–sectional plane and 64 CV in the spanwise direction. For a second '*fine*' grid (named **B**) the number of CV in the cross–sectional plane is doubled in both directions (x, y) leading to 325×325 CV, whereas the number of CV in the spanwise direction is kept constant (total of 6.76 million CV). Both grids have a spanwise extension of the integration domain $Z_{max} = 2D$ (except Run B4, see Table 1). The main objective of the present study was to investigate the effect of different SGS models for the high–Re case. Therefore, simulations based on the dynamic model (A1/B1), the Smagorinsky model with different Smagorinsky constants (A2/A3/B2) and no model (A4/B4) were carried out. Additionally, Table 1 gives an overview of a series of computations published earlier (Breuer, 1998b) which analyzed the influence of the spanwise extension of the integration domain. The difference between the grids named C1–3 and D1–3 is given by different spanwise extensions of the integration domain; for grids C1/D1 the spanwise length of the cylinder is only one cylinder diameter. For grids C2/D2 this length is doubled; however, the number of grid points is fixed, leading to elongated computational cells in the z–direction. Finally, for grids C3/D3 the spanwise extension is $\pi \times D$. At least the computed integral parameters were added to Table 1 in order to allow a rough comparison with the actual results. For all grids the entire integration domain has a radial extension of $15 \times D$ in the cross–section. The grid points are clustered in the wake region and in the vicinity of the cylinder ($\Delta r_{min}/D = 4\times10^{-4}$). Statistics are compiled over several vortex shedding cycles ($13 - 34$) and in the spanwise direction.

RESULTS AND DISCUSSION

Basic Flow Features

Before discussing the difference between the solutions obtained by different SGS models and on different grids, the basic flow features should be explained and compared with experimental observations. As expected from experiments, the LES computations of the sub–critical flow past the cylinder ($Re = 140,000$) exhibit the well known von Kármán vortex street with periodic vortex shedding. The Strouhal number St varies around 0.2 for most of the computations (see Table 1

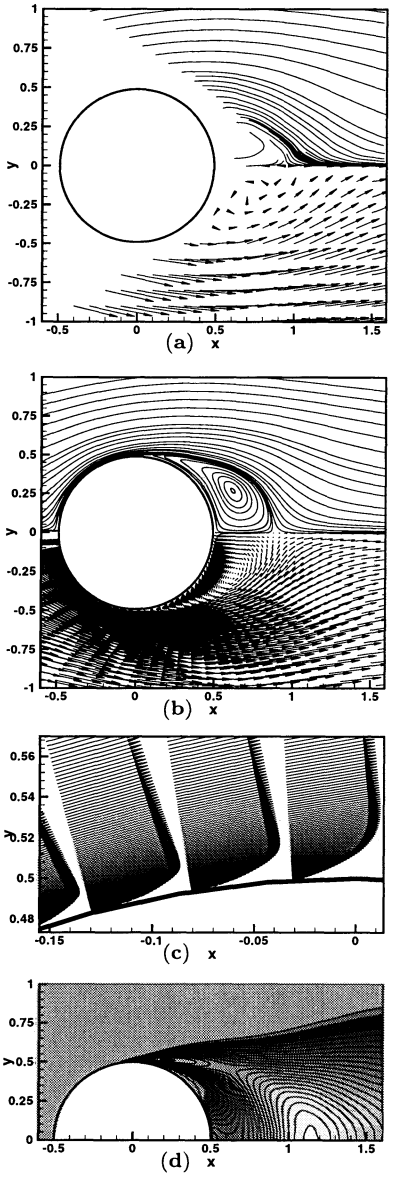

Figure 1: Time–averaged flow field for the sub–critical flow past a circular cylinder at $Re = 140,000$: (**a**) measurements by Cantwell and Coles (1983), (**b**) LES on fine grid (Run B2), (**c**) zoom of the boundary layer near apex of the cylinder, (**d**) contours of turbulent kinetic energy k.

Table 1: Overview of all high–Re simulations and computed integral parameters.

Run	Grid	Z_{max}	SGS Model	L_r/D	C_d	$C_{P_{back}}$	St	$\Theta_{Sep}(^o)$
Coarse Grid / Different SGS Models								
A1	$165 \times 165 \times 64$	$2D$	Dynamic	0.572	1.239	-1.398	0.204	96.37
A2	$165 \times 165 \times 64$	$2D$	Smago. $C_S = 0.1$	0.416	1.218	-1.411	0.217	95.16
A3	$165 \times 165 \times 64$	$2D$	Smago. $C_S = 0.065$	0.712	0.707	-0.677	0.247	94.58
A4	$165 \times 165 \times 64$	$2D$	–			divergent		
Fine Grid / Different SGS Models								
B1	$325 \times 325 \times 64$	$2D$	Dynamic	0.336	1.454	-1.764	0.204	95.00
B2	$325 \times 325 \times 64$	$2D$	Smago. $C_S = 0.1$	0.375	1.286	-1.480	0.203	92.59
B4	$325 \times 325 \times 64$	$1D$	–	0.654	0.388	-0.457	0.326	99.33
Coarse Grid / Different Domain Sizes								
C1	$165 \times 165 \times 64$	$1D$	Smago. $C_S = 0.1$	0.509	0.971	-1.083	0.235	96.60
C2=A2	$165 \times 165 \times 64$	$2D$	Smago. $C_S = 0.1$	0.416	1.218	-1.411	0.217	95.16
C3	$165 \times 165 \times 64$	πD	Smago. $C_S = 0.1$	0.462	1.276	-1.514	0.218	93.86
Fine Grid / Different Domain Sizes								
D1	$325 \times 325 \times 64$	$1D$	Smago. $C_S = 0.1$	0.413	1.057	-1.221	0.196	93.62
D2=B2	$325 \times 325 \times 64$	$2D$	Smago. $C_S = 0.1$	0.375	1.286	-1.480	0.203	92.59
D3	$325 \times 325 \times 64$	πD	Smago. $C_S = 0.1$	0.419	1.368	-1.600	0.205	91.45
Experiments								
Cantwell and Coles (1983)				≈ 0.44	1.237	-1.21	0.179	
Wieselsberger et al. (1923), Achenbach (1968), Son & Hanratty (1969), Zdravkovich (1997), Fey et al. (1998)					≈ 1.2		≈ 0.2	(see text)

for exceptions). Cantwell and Coles (1983) found an extremely low Strouhal number $St = 0.179$, which, however, is not in good agreement with most of the other experimentally determined St values, tending towards $St \approx 0.2$ (e.g., Son and Hanratty, 1969; Zdravkovich, 1997; Fey et al., 1998). This deviation from the consensus of other experiments was mentioned by the authors themselves. Especially the predicted St values based on the dynamic (A1/B1) and the Smagorinsky model with $C_S = 0.1$ (A2/B2) agree fairly well with the generally accepted St value.

Figure 1 shows a first qualitative comparison of the streamlines and vector field obtained by averaging the instantaneous flow field in time and in the spanwise direction. As an example, Run B2 (fine grid, Smagorinsky model) is compared with the experimental data of Cantwell and Coles (1983). Unfortunately, no measurements were taken for the front part of the cylinder and in the direct vicinity of the rear. However, in accordance with the experimental data the LES computation predicts an attached recirculation region behind the cylinder (recirculation length L_r) which is much shorter than for $Re = 3900$ (Breuer, 1998a). In contrast to $Re = 3900$, no small counter–rotating vortices attached to the backward side of the cylinder can be observed at the present Re. The primary separation angle Θ_{Sep} is included in Table 1. It decreases with the spanwise elongation of the grid and with the resolution in the cross–sectional plane. The lowest value of $\Theta_{Sep} = 91.45^o$ is found for Run D3, which means that the separation point is still behind the apex of the cylinder. Owing to the extremely thin boundary layer at the cylinder, the determination of the time–averaged separation point on the surface is exceedingly difficult in experiments. Cantwell and Coles (1983) provided a value for the inflection point of the mean pressure coefficient of about 77^o, which, however, is not equal to the separation angle. In another experimental investigation by Son and Hanratty (1969), a value of $\Theta_{Sep} = 78^o$ was determined at $Re = 10^5$. A very interesting observation was made by Achenbach (1968). At $Re = 10^5$ (sub–critical flow) he found that the boundary layer separates laminarly at $\Theta_{Sep} = 78^o$. Just before transition into the critical region at $Re = 2.6 \times 10^5$ the boundary layer is still laminar and separates at an angle $\Theta_{Sep} = 94^o$. At $Re = 1.5 \times 10^5$ Achenbach (1968) found a minimum for the separation angle of $\Theta_{Sep} = 72^o$, indicating a highly non–linear relationship between the separation angle and the Reynolds number in this Re range.

Fig. 1 (c) shows a zoom of the time–averaged velocity field in the vicinity of the apex of the cylinder. The thin boundary layer is resolved in this region by about 25–30 grid points on the fine grid. In order to prove that the boundary layer separates laminarly, one possibility is to consider the predicted distribution of the turbulent kinetic energy k (Fig. 1 (d)), which clearly demonstrates that k is zero up to the apex of the cylinder. Hence separation takes place in the laminar mode as experimentally expected for a sub–critical Re forming free shear layers. An immediate transition to turbulence close to the cylinder is observed accompanied by a very short recirculation region. Compared with the low–Re case, transition to turbulence moves further upstream.

Influence of SGS Model and Resolution

Table 1 gives an overview of all simulations carried out. Focusing on simulations A1–4 and B1–4, the influence of different SGS models and different resolutions can be investigated. Therefore, some computed integral parameters are listed in Table 1: the recirculation length L_r/D, the drag coefficient C_d, the back–pressure coefficient $C_{P_{back}}$, the Strouhal number St and the separation angle Θ_{Sep}.

First, the importance of SGS modeling for high–Re flows is clearly demonstrated by Run A4 without any

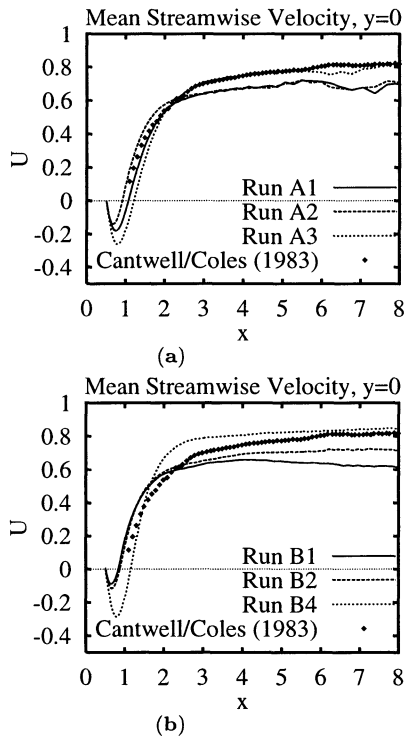

Figure 2: Time–averaged streamwise velocity U along the symmetry line $y = 0$ for different SGS models: (**a**) coarse grid, Runs A1–3; (**b**) fine grid, Runs B1–4.

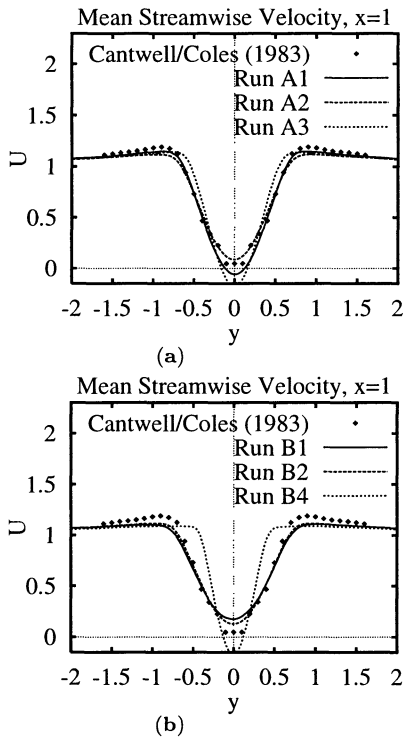

Figure 3: Time–averaged streamwise velocity U along a constant x–position $x = 1$ for different SGS models: (**a**) coarse grid, Runs A1–3; (**b**) fine grid, Runs B1–4.

SGS model. On the coarse grid (A4) it was not possible to achieve a solution at all. Grid refinement (B4) leads to a non–diverging solution; however, large deviations of all integral parameters are observed for this case compared with other simulations and experiments, e.g. the drag coefficient is only about one third of the experimental value and the St value is much too high. Based on *numerical experiments* performed for the low–Re case (Breuer, 1998a) showing only a small influence of SGS modeling on the predicted results, this example emphasizes the increasing importance of SGS models with increasing Re. Especially for low diffusive numerical schemes such as CDS, the SGS model has to ensure energy dissipation in the smallest scales leading to a stabilizing effect for the numerical solution.

For a more detailed comparison of the time–averaged flow field, profiles of the velocity components are plotted. First, the results along the symmetry axis ($y = 0$) of the cylinder are considered. Fig. 2 (a) shows the streamwise velocity U for different SGS models on the coarse grid (A1–3), whereas the results for the fine grid (B1–4) are shown in Fig. 2 (b). The experimental data of Cantwell and Coles (1983) are shown as symbols. On the coarse grid the Smagorinsky model with $C_S = 0.1$ (A2) leads to a slightly underpredicted recirculation length and a drag coefficient which deviates only 1.5% from the value given by Cantwell and Coles. The St value is about 8% too high. The effect of a decreasing C_S value is demonstrated by Run A3 with $C_S = 0.065$. Similarly to the case without any model L_r and St are too large and C_d is much too small. It should be mentioned that the present reduction of C_S from 0.1 to 0.065 leads to $\approx$ 2.4 times smaller turbulent eddy viscosity values in the model. The dynamic model (A1) predicts a larger recirculation length than the experiment and only small deviations from A2 occur for the other integral parameters. In the near wake the agreement with the experimental velocity distribution is satisfactory. However, the deviations increase with increasing distance from the cylinder. In the far wake the streamwise velocity for A1 and A2 is too low compared with the experimental data. On the refined grid both models (B1/B2) show shorter recirculation lengths and higher C_d values. The changes from the coarse to the fine grid are more emphasized for the dynamic model (A1 $\rightarrow$ B1). With the exception of Run B4 the streamwise velocity in the far wake is too small.

Figs. 3 and 4 show the time–averaged streamwise velocity U and the normal component V in the near wake along a constant x–position ($x = 1$). For comparison the data of Cantwell and Coles (1983) are added again. Taking into account only the results of A1/A2 and B1/B2, minor deviations occur for the U–profiles. In general, the agreement with the measurements is satisfactory. For the normal velocity V the results based on different SGS models and different resolutions are even closer to each other. They agree fairly well with the experimental data at this position. Further downstream (e.g., $x = 3$) the profiles of the streamwise velocity U (not shown here) still coincide fairly well with the measured data. The maximum normal velocity V at this position in the flow field has already dropped to about 4% of u_∞. Therefore, it is difficult to capture by simulation. All LES computations slightly underpredict

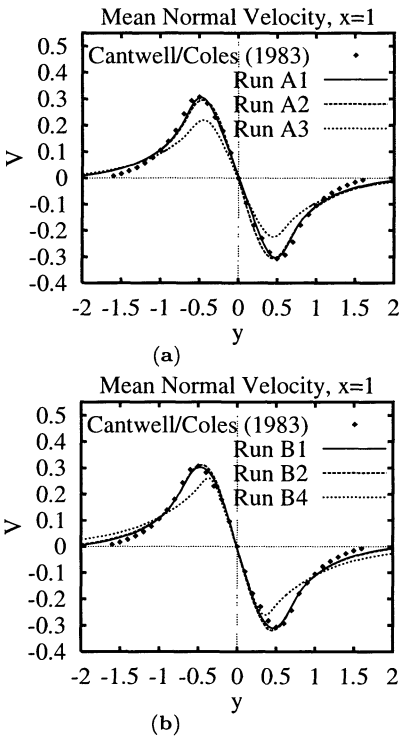

Figure 4: Time–averaged normal velocity V along a constant x–position $x = 1$ for different SGS models: (**a**) coarse grid, Runs A1–3; (**b**) fine grid, Runs B1–4.

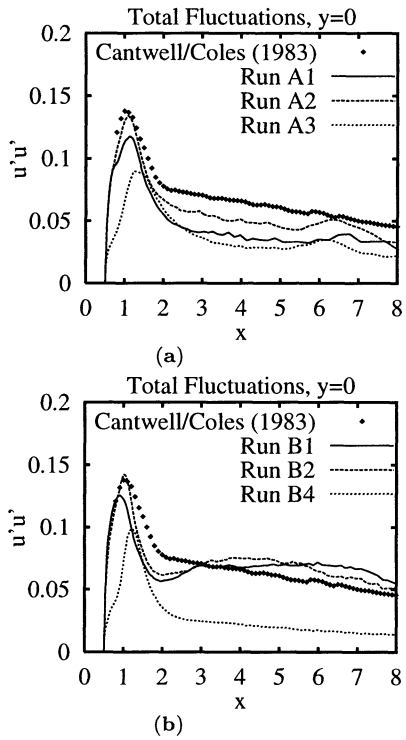

Figure 5: Total resolved streamwise Reynolds stress $\overline{u'u'}$ along the symmetry line $y = 0$ for different SGS models: (**a**) coarse grid, Runs A1–3; (**b**) fine grid, Runs B1–4.

this velocity component. Owing to the clustering of the grid points in the vicinity of the cylinder, the resolution (even of grid B) deteriorates on moving further downstream. This results in an unsatisfactory reproduction of the velocity defect in the far wake of the cylinder ($x > 5$), as already shown in Fig. 2.

Additionally to the mean flow field, higher order moments have been investigated. In Fig. 5 the total resolved streamwise Reynolds stress $\overline{u'u'}$ along the symmetry line ($y = 0$) is plotted. The symbols represent the sum of the periodic and turbulent fluctuations calculated from the measured data of Cantwell and Coles (1983). The agreement for this stress component (excluding A3 and B4) is good, especially in the near wake. The position of the peak value at $x \approx 1$, which almost corresponds to the recirculation length, and the peak value itself are well reproduced by both models. On both grids the Smagorinsky model (A2/B2) provides a higher peak value than the dynamic model (A1/B1). Deviations occur in the far wake of the cylinder, whereas the level of $\overline{u'u'}$ is much better predicted on the fine grid (B1/B2).

In contrast to this good agreement of $\overline{u'u'}$ along the symmetry axis, the cross–stream Reynolds stress shown in Fig. 6 is highly overpredicted for A1–2 and B1–2, where the deviations are even emphasized on the fine grid (B1–2). The dynamic model on the fine grid (B1) produces the highest peak value. In general, the positions of the computed maxima are too close to the cylinder and the peak values are much too high. In this context, it is interesting that a similar observation was made for the low–Re case (Breuer, 1998a). Also in this case the streamwise component $\overline{u'u'}$ was more accurately predicted than the cross–stream component $\overline{v'v'}$ and the deviations of $\overline{v'v'}$ even increase by grid refinement.

Finally, in Fig. 7 the shear stress $\overline{u'v'}$ is plotted along a constant x–position ($x = 1$) in the near wake region. Especially for Run A1 with the dynamic model the results are in close agreement with the measurements, whereas the Smagorinsky model (A2) slightly overpredicts the peak values. As observed before, grid refinement does not automatically lead to improved results. Again contrary to expectations, the agreement between the LES results and the measurements deteriorates on the finer grid (B1/B2), not shown here. This behavior is not understood.

CONCLUSIONS

The present work has demonstrated that LES of practically relevant high–Re flows should become feasible in the near future. As a test case involving remarkably complex flow features, the flow past a circular cylinder was computed at $Re = 140,000$. Because the resolution cannot be enlarged according to the ratio of the largest to the smallest length scales ($Re^{9/4}$), the SGS model has to take a wider spectrum of turbulent vortices into account. As expected, this leads to the prime importance of SGS modeling being insignificant for low Re. Both the Smagorinsky and the dynamic model were applied. Furthermore, simulations without any model were carried out, clearly emphasizing the above state-

ment. It was shown that the dynamic model works well for high–Re complex flows. However, the superiority of the dynamic model over the Smagorinsky model could not be definitely proved, with the exception that no proper Smagorinsky constant has to be chosen. An astonishing outcome was that grid refinement did not automatically lead to improved results for all quantities. In general, the LES results were in satisfactory agreement with the experimental data, especially in the near wake. Owing to the coarse resolution in the far wake, larger deviations were observed here. Particularly for flows involving large–scale vortex motion, LES is becoming an attractive alternative to Reynolds–averaged turbulence modeling also for high–Re.

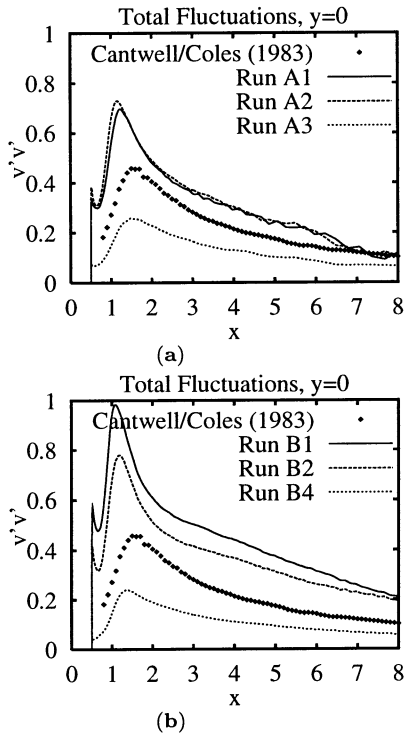

Figure 6: Total resolved cross–stream Reynolds stress $\overline{v'v'}$ along the symmetry line $y = 0$ for different SGS models: (**a**) coarse grid, Runs A1–3; (**b**) fine grid, Runs B1–4.

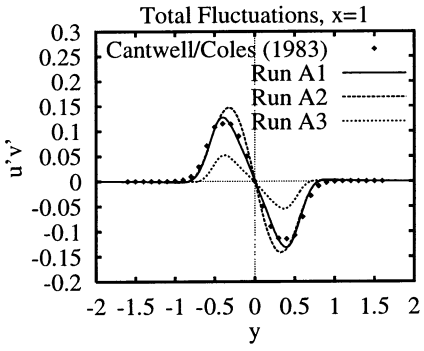

Figure 7: Total resolved shear stress $\overline{u'v'}$ along a constant x–position $x = 1$ for different SGS models, Runs A1–3.

REFERENCES

Achenbach, E., 1968, "Distribution of Local Pressure and Skin Friction Around a Circular Cylinder in Cross–Flow up to $Re = 5 \times 10^6$", *J. Fluid Mechanics*, Vol. 34, part 4, pp. 625–639.

AGARD–AR–345, 1998, "A Selection of Test Cases for the Validation of Large–Eddy Simulations of Turbulent Flows", *AGARD Advisory Report*, No. 345.

Breuer, M., and Rodi, W., 1994, "Large–Eddy Simulation of Turbulent Flow Through a Straight Square Duct and a 180° Bend", *Fluid Mech. and its Appl.*, Vol. 26, pp. 273–285, *Direct and Large–Eddy Simulation I, First ERCOFTAC Workshop on DNS & LES*, Guildford, Surrey, U.K., 27–30 March 1994, eds. P.R. Voke, L. Kleiser & J.P. Chollet, Kluwer Academic, Dordrecht.

Breuer, M., and Rodi, W., 1996, "Large–Eddy Simulation of Complex Turbulent Flows of Practical Interest", In: 'Flow Simulation with High–Performance Computers II', ed. E.H. Hirschel, *Notes on Numerical Fluid Mechanics*, Vol. 52, pp. 258–274, Vieweg Verlag.

Breuer, M., 1998a, "Large Eddy Simulation of the Sub–Critical Flow Past a Circular Cylinder: Numerical and Modeling Aspects", *Int. J. Numerical Methods in Fluids*, Vol. 28, pp. 1281–1302.

Breuer, M., 1998b, "Large Eddy Simulation of High Reynolds Number Circular Cylinder Flow",, *Proc. of the Workshop on Industrial and Environmental Applications of Direct and Large Eddy Simulation*, August 5–7, 1998, Boğaziçi University, Istanbul, Turkey, *Lecture Notes in Physics*, Springer Verlag, Berlin, in press.

Cantwell, B., and Coles, D., 1983, "An Experimental Study on Entrainment and Transport in the Turbulent Near Wake of a Circular Cylinder", *J. Fluid Mech.*, Vol. 136, pp. 321–374.

Fey, U., König, M., and Eckelmann, H., 1998, "A New Strouhal–Reynolds Number Relationship for the Circular Cylinder in the Range $47 < Re < 2 \cdot 10^5$", *Phys. Fluids A*, Vol. 10 (7), pp. 1547–1549.

Germano, M., Piomelli, U., Moin, P., Cabot, W.H., 1991, "A Dynamic Subgrid Scale Eddy Viscosity Model", *Phys. Fluids A*, Vol. 3 (7), pp. 1760–1765.

Lilly, D.K., 1992, "A Proposed Modification of the Germano Subgrid–Scale Closure Method", *Phys. Fluids A*, Vol. 4 (3), pp. 633–635.

Rodi, W., Ferziger, J.H., Breuer, M., and Pourquié, M., 1997, "Status of Large Eddy Simulation: Results of a Workshop", *Workshop on LES of Flows Past Bluff Bodies*, Rottach–Egern, Tegernsee, Germany, June 26–28, 1995, *J. Fluids Eng.*, Vol. 119, no. 2, pp. 248–262.

Son, J.S., and Hanratty, T.J., 1969, "Velocity Gradients at the Wall for Flow Around a Cylinder at Reynolds Numbers from 5×10^3 to 10^5", *J. Fluid Mechanics*, Vol. 35, part 2, pp. 353–368.

Voke, P.R., 1997, "Flow Past a Square Cylinder: Test Case LES2", *Proc. of the 2nd ERCOFTAC Workshop on Direct and Large–Eddy Simulation*, Grenoble, France, September 16–19, 1996, *ERCOFTAC Series*, Vol. 5, pp. 355–373, *Direct and Large–Eddy Simulation II*, eds. J.P. Chollet, P.R. Voke and L. Kleiser, Kluwer Academic, Dordrecht.

Wieselsberger, C., Betz, A., and Prandtl, L., 1923, "Versuche über den Widerstand gerundeter und kantiger Körper", *Ergebnisse AVA Göttingen*, pp. 22–32.

Zdravkovich, M.M., 1997, "Flow Around Circular Cylinders, Vol. 1: Fundamentals", Oxford University Press, New York.